SPIRE-UCF-PUB-001694

SPIRE - Herschel's Submillimetre Camera and Spectrometer

Matthew Griffin[a], Bruce Swinyard[b], Laurent Vigroux[c]
[a]Department of Physics and Astronomy, University of Wales, Cardiff, Queens Buildings, 5 The Parade, Cardiff CF24 3YB, UK.
[b]Rutherford Appleton Laboratory, Chilton, Didcot, Oxfordshire OX11 0QX, England.
[c]CEA-Service d'Astrophysique, Bât. 709, Orme des Merisiers, 91191 Gif sur Yvette, France.

ABSTRACT

SPIRE, the Spectral and Photometric Imaging Receiver, will be an imaging photometer and spectrometer for ESA's Herschel Space Observatory. The main scientific goals and design drivers for SPIRE are deep extragalactic and galactic imaging surveys and spectroscopy of star-forming regions in own and nearby galaxies. It comprises a three-band imaging photometer with bands centred at approximately 250, 360 and 520 μm, and an imaging Fourier Transform Spectrometer (FTS) covering 200-670 μm. The detectors are feedhorn-coupled NTD spider-web bolometers cooled to 300 mK by a recyclable ^{3}He refrigerator with a cycle time of less than two hours and a hold time of more than 46 hours. The photometer field of view is 4 x 8 arcminutes (the largest that can be accommodated) and is observed simultaneously in the three spectral bands. The angular resolution is determined by the telescope diffraction limit, with FWHM beam widths of approximately 17, 24 and 35 arcseconds at 250, 360 and 520 μm, respectively. An internal beam steering mirror allows spatial modulation of the telescope beam, and mapping observations can also be made by drift-scanning the telescope. The FTS has a field of view of 2.6 arcminutes. It uses a dual-beam configuration with novel broad-band intensity beam dividers to provide high efficiency and separated output and input ports. The FTS scanning mirror has a linear travel of up to 3.5 cm, providing adjustable spectral resolution of 0.04-2 cm^{-1} ($\lambda/\Delta\lambda$ = 20 - 1000 at 250 μm). The instrument design, operating modes, and estimated sensitivity are described.

Keywords: Herschel, Far Infrared, Submillimetre, Bolometer, Instrumentation

1 INTRODUCTION

The Spectral and Photometric Imaging Receiver, SPIRE, is one of three scientific instruments to fly on ESA's Herschel Space Observatory [1]. The main scientific goals and design drivers for SPIRE are the investigation of the statistics and physics of galaxy and structure formation at high redshift and the study of the early stages of star formation. These scientific projects require large-area (tens of square degrees) deep imaging surveys at far-infrared and submillimetre wavelengths, and follow up of these surveys with spectroscopy of selected sources. SPIRE will exploit the particular advantages of Herschel: its large-aperture, cold, low-emissivity telescope; the lack of atmospheric emission and attenuation giving access to the poorly explored 200-700-μm range, and the large amount of high quality observing time.

Galaxies emit a large fraction (from 30% to nearly 100%) of their luminosity in the far infrared (FIR) due to re-processing of stellar UV radiation by interstellar dust grains. The FIR peak is redshifted into the SPIRE wavelength range for galaxies with redshift, z, greater than ~ 1. Determining the total luminosity of a galaxy requires measurement of its Spectral Energy Distribution (SED). The study of the early stages of galaxy evolution thus needs an instrument that can detect emission from high-z galaxies in the submillimetre, enabling their SEDs and luminosities to be derived. The pioneering observations made with the SCUBA submillimetre camera on the JCMT have emphasised the importance of the FIR-submillimetre band for studies of the high-redshift universe[2].

[a] Further author information: E-mail: matt.griffin@astro.cf.ac.uk; Telephone: +44-(0)29-2087-4203; Fax: +44-(0)29-2087-4056

Star formation occurs by the fragmentation and collapse of dense cloud cores in the interstellar medium (ISM), and the very first stages of this process are not well understood. FIR and submillimetre observations with high spatial resolution are needed to make complete surveys of protostellar clumps to determine their bolometric luminosities and mass function. SPIRE and the other Herschel instruments will also, for the first time, enable astronomers to observe at high spatial resolution the physical and chemical conditions obtaining in the cold parts of the ISM and to study the behavior of the interstellar gas and dust before and during star formation. SPIRE's high sensitivity to cold dust emission also makes it an ideal instrument to study the material that is ejected in large quantities from evolved stars, enriching the interstellar medium with heavy elements. Significant amounts of matter - as yet undetected - are ejected from stars before the white dwarf stage. These mass loss phases need to be characterised to complete theories of stellar evolution, and of the heavy element enrichment of the galaxy. Star formation and the interaction of forming and evolved stars with the ISM are also, of course, intimately related to galaxy formation and evolution, which occur through just these processes.

These are high priority programmes for Herschel, and require sensitive continuum imaging in several bands to carry out surveys, and a low-resolution spectroscopic mode to obtain detailed SEDs of selected objects and measure key spectral lines. Although the SPIRE design has been dictated by these two main scientific programmes, it will offer the astronomical community a powerful tool for many other astrophysical studies: giant planets, comets, the galactic interstellar medium, nearby galaxies, ultraluminous infrared galaxies, and active galactic nuclei. Its capabilities will remain unchallenged by the ground-based and the airborne observatories which are planned to come into operation over the next decade.

In this paper we present an update on the SPIRE instrument design, which has been refined and improved since its description[3] at the Munich SPIE meeting in 2000.

2 INSTRUMENT OVERVIEW

SPIRE contains a three-band imaging photometer and an imaging Fourier Transform Spectrometer (FTS), both of which use 0.3-K feedhorn-coupled "spider-web" NTD germanium bolometers cooled by a ^{3}He refrigerator. The photometer and spectrometer do not operate simultaneously. The photometer field of view is 4 x 8 arcminutes, the largest that can be achieved given the location of the SPIRE field of view in the Herschel focal plane and the size of the telescope unvignetted field of view. Three feedhorn-coupled bolometer arrays are used for broad-band photometry ($\lambda/\Delta\lambda \approx 3$) in three wavelength bands centred on approximately 250, 360 and 520 μm, which are designated PSW, PMW and PLW, respectively. The PMW band is designed to be near identical the corresponding Planck-HFI channel in order to facilitate accurate cross-calibration of Herschel and Planck observations. The same field of view is observed simultaneously in the three bands through the use of fixed dichroic beam-splitters. Spatial modulation can be provided either by a two-axis Beam Steering Mirror (BSM) or by scanning the telescope across the sky. An internal thermal source is available to provide a repeatable calibration signal for the detectors. The FTS uses novel broadband intensity beam dividers, and combines high efficiency with spatially separated input ports. One input port covers a 2.6-arcminute diameter field of view on the sky and the other is fed by an on-board reference source. Two bolometer arrays are located at the output ports, one covering 200-325 μm and the other 315-670 μm. The FTS moving mirror drive mechanism can be operated in either continuous scan or step-and-integrate mode. The spectral resolution, as determined by the total optical path difference, will be adjustable between 0.04 and 2 cm^{-1} (corresponding to $\lambda/\Delta\lambda$ = 1000 - 20 at 250 μm wavelength).

The focal plane unit is approximately 700 x 400 x 400 mm in size, and has three separate temperature stages at nominal temperatures of 4.5 K, 1.7 K (provided by the Herschel cryostat) and 0.3 K (provided by SPIRE's internal cooler). The main 4.5-K structural element of the FPU is an optical bench panel which is supported from the 10-K cryostat optical bench by stainless steel mounts. The photometer and spectrometer are located on either side of this panel. Most of the instrument optics are at 4.5 K, but the detector arrays and final optics are contained within 1.7-K enclosures. The ^{3}He refrigerator cools all of the five detector arrays to 0.3 K. Two JFET preamplifier modules are used to read out the bolometer signals, one for the photometer and one for the spectrometer. The JFET units are attached to

the 10-K optical bench close to the 4.5-K enclosure, with the JFETs heated internally to their optimum operating temperature of ~ 120 K.

The SPIRE warm electronics consist of three units: the Detector Control Unit (DCU), provides bias and signal conditioning for the arrays and cold readout electronics, and reads out the detector signals; the FPU Control Unit (FPU) controls the FPU mechanisms and the ^{3}He cooler, and reads out all FPU thermometers; and the Digital Processing Unit (DPU) acts as the interface to the spacecraft for instrument commanding, and telemetry to Earth.

3 IMAGING PHOTOMETER

3.1 OPTICS AND FPU DESIGN

Optics: Figure 1 shows the photometer layout. The 4.5-K optics are mounted directly from the optical bench panel. The 1.7-K enclosure is supported from the panel by stainless steel supports, and contains the detector arrays, the dichroics and fold mirrors. The three array modules are bolted to the outside wall of the 1.7-K box. Within each bolometer array module, the detector arrays, feedhorns and the final filter are thermally isolated from the 1.7-K structure by tensioned Kevlar threads, and are cooled by a thermal strap to the ^{3}He refrigerator (see Section 5). The photometer input optics are shared with the spectrometer. The separate spectrometer field of view is directed to the other side of the optical bench panel by a pick-off mirror.

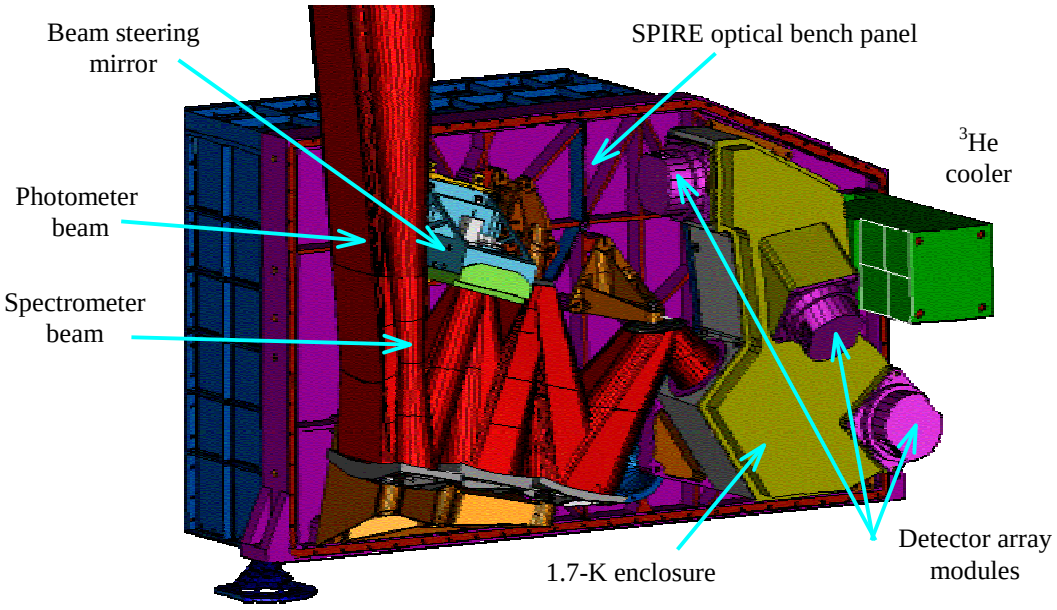

Figure 1: Computer-generated image of the SPIRE photometer layout.

The photometer optical design is illustrated in Fig. 2, and is described in more detail by Dohlen et al.[4] It is an all-reflective system except for two dichroics used to direct the three wavelength bands onto different bolometer arrays, and various filters used to define the pass-band and reject out-of-band radiation. The design achieves close to diffraction-limited imaging across the whole 4 x 8 arcminute field of view, which is offset by 11 arcminutes from the centre of the Herschel telescope's highly curved focal surface. Mirror M3 lies below the focus, and receives the f/8.68 Herschel telescope beam and forms an image of the telescope secondary at the flat beam steering mirror, M4. Mirror M5 converts the focal ratio to f/5 and provides an intermediate focus at M6, which re-images the pupil at M4 to a cold stop. M7, M8 and M9 constitute a one-to-one optical relay to bring the M6 focus to the three detector arrays. The

beams for the three bands are directed onto the arrays at f/5 by a combination of flat folding mirrors and fixed dichroics. M3 - M8 are at 4.5 K and the cold stop and all subsequent optics are at 1.7 K.

Internal source: An internal thermal source[5] provides a repeatable signal for the bolometer arrays. It is not required to provide an absolute calibration of the system - that will be done using observations of standard astronomical sources. The source radiates through a hole in the centre of the beam steering mirror, M4, occupying a central area contained within the region of the pupil obscured by the hole in the primary mirror. With a brightness temperature of 40 K and an emitting area of 1 mm diameter compared to the pupil diameter of approximately 30 mm, the source will produce a power at the detector of approximately $[40/(0.04 \times 80)](1/30)^2 \approx 1.4\%$ of the telescope background power. The latter is typically a few pW, so the signal level provided by the thermal source is a few x 10^{-14} W. With a detector NEP of a few x 10^{-17} W $Hz^{-1/2}$, this provides a very large instantaneous S/N. As M4 is at a pupil image, the illumination is close to uniform over the arrays. The device is essentially an inverse bolometer. The emitter is a 1 x 1 mm NiCr coated Mica chip suspended from the 4.5-K housing by 25-μm diameter brass wires. These wires are soldered on a glass fibre PC board. Current passed through the metal film heats it up to a temperature of 40 K or more. The typical resistance is 300 Ω, requiring ~ 2.5 mA drive current for 2 mW power. Prototype devices tested to date show that the radiant output and time constant requirements can be met comfortably with this level of applied power.

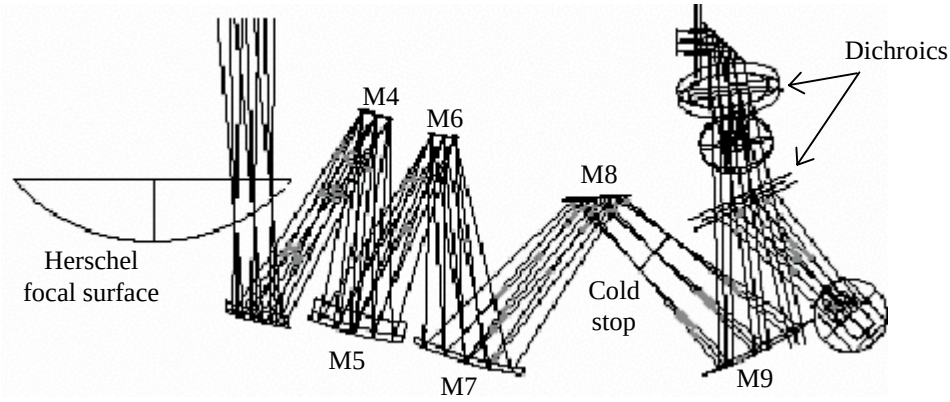

Figure 2: SPIRE photometer optical design.

Beam steering mechanism: The beam steering mirror, M4, can chop ± 2 arcminutes along the long axis of the 4 x 8 arcminute field of view, at frequencies up to 2 Hz with an efficiency of > 90%. and power dissipation < 2 mW. It can operate at higher frequencies if necessary with reduced efficiency and increased power dissipation. The mechanism can simultaneously chop at up to 1 Hz in the orthogonal direction by up to 30 arcseconds. Two axis motion allows "jiggling" of the pointing to create a fully sampled image of the sky with the feedhorn-coupled detectors whose diffraction-limited beams on the sky are separated by approximately twice the beam FWHM. Flex pivots allow the necessary rotations of the mirror about the chop and the jiggle axes while constraining translational movement. The pivots have high radial stiffness, virtually eliminating unwanted rotation of the mirror due to bearing flexibility. They have negligible static friction, simplifying the design of the control system and minimising the power demand on the actuators. This restoring force of the pivots ensures that the mirror returns to the neutral position in the event of power failure to the mechanism actuators. The beam steering mechanism is described in more detail by Pain et al.[6]

Filters and dichroics: The SPIRE filtering scheme provides precise definition of the spectral passbands with high out-of-band rejection and maximum in-band transmission, and also minimises the thermal loading on the low-temperature stages by reflecting short-wavelength radiation. To achieve complete rejection out to UV wavelengths, four blocking filters are needed in the chain. The bands are defined by a combination of transmission edges (of filters in front of the detectors), reflection/transmission edges of the dichroics, and the cutoff wavelengths of the feedhorn output waveguides. The three bands are centred at 250, 363 and 517 μm, respectively, with resolution ($\lambda/\Delta\lambda$) of 3.0, 3.2, and 3.0, respectively. Figure 3 shows the measured transmission profiles of a representative filter set, with properties similar to the SPIRE PMW design.

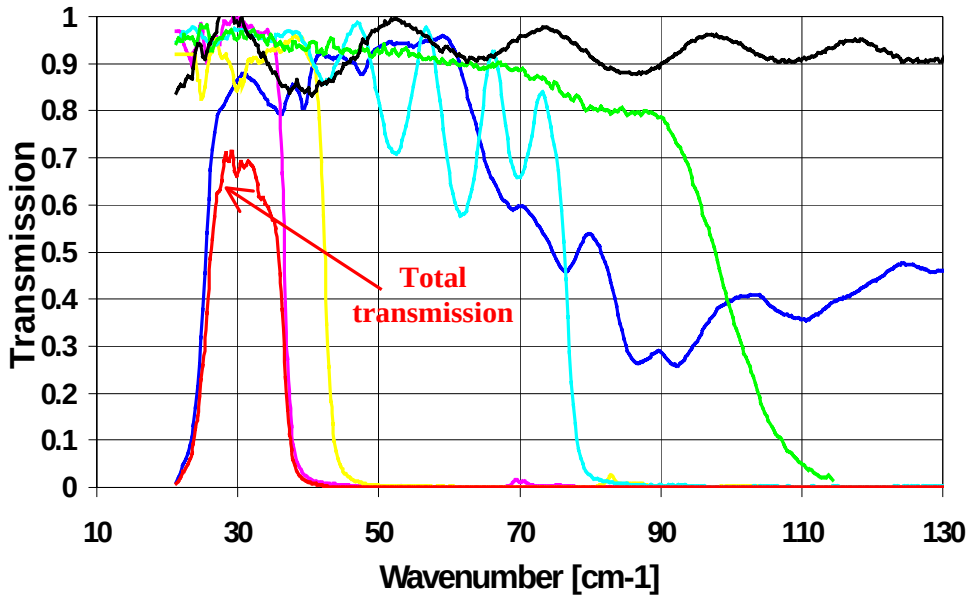

Figure 3: Transmission of a prototype filter set similar to the SPIRE PMW band. The transmissions of the individual elements have been measured separately and multiplied together to derive the overall transmission.

Detector arrays: The detectors are spider-web bolometers using NTD germanium thermometers[7], coupled to the telescope by hexagonally close-packed 2Fλ-diameter single-mode conical feedhorns, giving diffraction limited beams of FWHM 17, 25 and 35 arcseconds for the PSW, PMW and PLW bands respectively. The arrays contain 43 (PLW), 88 (PMW) and 139 (PSW). The photometer arrays are shown schematically in Fig. 4a, and Fig. 4b is a photograph of a prototype array module. Each array unit has an interface to the 1.7-K box and a thermal strap from the ^{3}He cooler to the 0.3-K stage, which is supported by Kevlar strings from the 1.7-K level. Electrical connections to the detectors are made with Kapton ribbon cables within the array modules and with woven manganin cables between the arrays and the JFETs. The bolometers are AC-biased at a frequency of around 100 Hz, eliminating 1/f noise from the JFET readout, and giving a 1/f knee for the system of less than 100 mHz. Conservative estimates of the bolometer Detective Quantum Efficiency (DQE) vary between 0.6 and 0.7 ensuring that the overall NEP will be dominated by the thermal emission from the telescope.

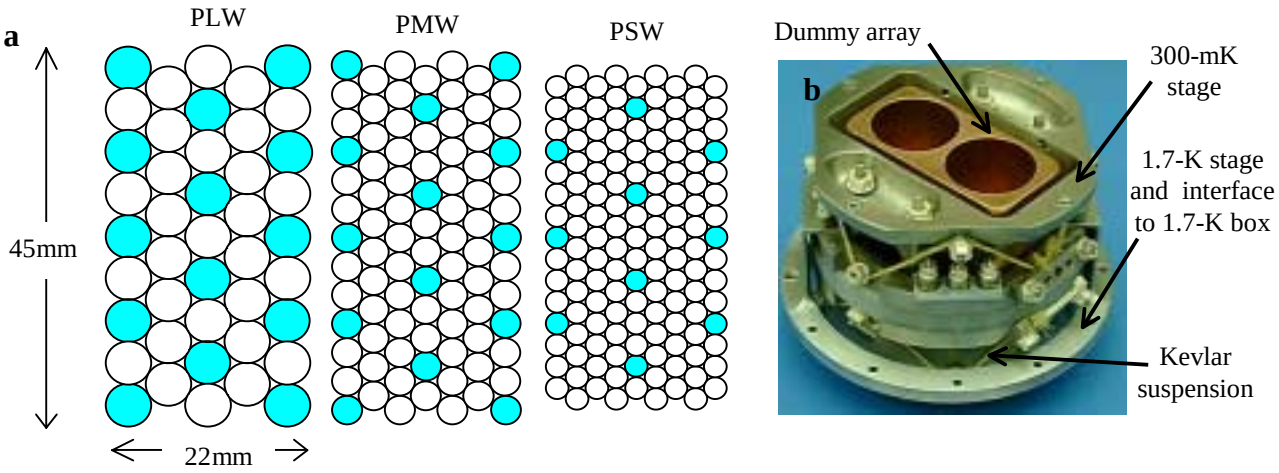

Figure 4: (a) Layout of the photometer arrays. The shaded detectors are those for which there is exact overlap on the sky for the three bands; (b) SPIRE detector array module mechanical prototype.

3.3 PHOTOMETER OBSERVING MODES

The photometer will have three principal observing modes, as illustrated in Fig. 5 and described below.

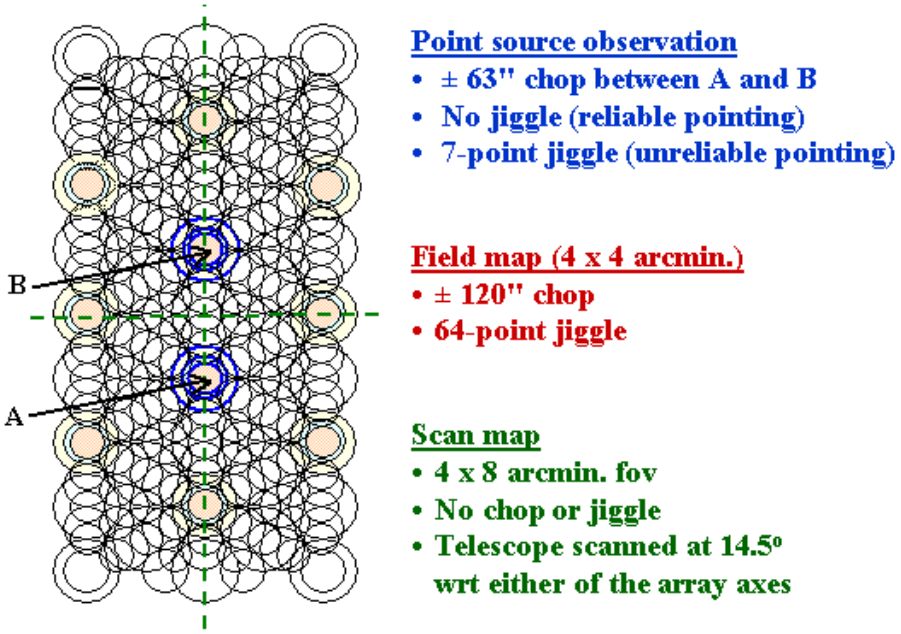

Figure 5: Photometer observing modes

Point or compact source photometry: Chopping will be used in this case. There are several sets of three detectors for which the beams at the three wavelengths are exactly co-aligned on the sky (indicated by the shaded circles in Fig. 4). By chopping through the appropriate angle (126 arcseconds), three-band photometry can be carried out with maximum efficiency: the source is being observed in each band by one detector at all times. It may be necessary to ensure that positional errors due to telescope pointing inaccuracy or imperfect knowledge of the source position do not affect the accuracy of the measurement. In that case the beam steering mirror can be used to implement a seven-point mapping routine. With an angular offset of 6" for the seven-point, the S/N loss for a given integration time varies between 6% (PLW) and 20% (PSW), which is a small penalty to pay for assurance that pointing or source position errors do not result in an underestimate of the source flux density.

Field mapping: For mapping of regions a few arcminutes in size, the beam steering mirror will be used to carry out a jiggle map, similar to the mode of operation of the SCUBA bolometer camera on the JCMT[6]. A 64-point jiggle pattern is needed to achieve full spatial sampling in all bands simultaneously, with a step size of 9 arcseconds (half-beam spacing at 250 μm). A maximum field size of 4 x 4 arcminutes is available in this mode as the 2-arcminute regions at each end of the array will be chopped outside the field of view admitted by the photometer optics.

Scan mapping: This mode will be used for mapping large areas of sky (much bigger than the SPIRE field of view), including deep survey observations. The telescope will be scanned across the sky (at up to 1 arcminute per second, the maximum rate that the spacecraft can provide). Because of the excellent 1/f stability of the NTD detectors, the beam steering mirror does not need to be operated - signal modulation is provided by the telescope motion. To provide the necessary beam overlap for full spatial sampling over the strip defined by a single scan, the scan angle must be 14.5^{o} with respect to one of the array axes.

The available telemetry rate of 130 kbs allows all of the 270 photometer detectors to be sampled with 16-bit resolution at up to 28 Hz and the data telemetered directly to the ground with no on-board processing.

4 IMAGING FOURIER TRANSFORM SPECTROMETER

4.1 OPTICS AND FPU DESIGN

The FTS[9] uses two broadband, high-efficiency, intensity beam splitters in a Mach-Zehnder configuration rather than the traditional polarising beam dividers. This configuration has the advantage that all four ports are separately accessible, as in the classical Martin Puplett (M-P) polarising FTS. But the throughput is a factor of two higher than for the M-P as none of the incoming radiation is rejected, and there is no sensitivity to the polarisation of the incident beam. The performance of the beam dividers and of a bench-top implementation of this design has been demonstrated[10]. A thermal source is located at a pupil image in the second input port of the FTS, and provides a thermal spectrum that mimics the dilute 80-K black body emission spectrum of the telescope. This allows the large telescope background to be nulled, thereby reducing the dynamic range requirements for the detector sampling when the spectrometer is operated in continuous scan mode. The two FTS detector arrays are placed in the two output ports, with bands of 200-325 μm and 315-670 μm defined by a combination of filters and feedhorn waveguide cutoff. A single back-to-back moving roof-top mechanism serves both arms of the interferometer, with a frictionless carriage mechanism using double parallelogram linkage and flex pivots. The scan mirror position readout uses a Heidenhain Moiré fringe sensing system.

Optics: The focal plane layout of the FTS is shown in Fig. 6 and the optical design is illustrated in Fig. 7.

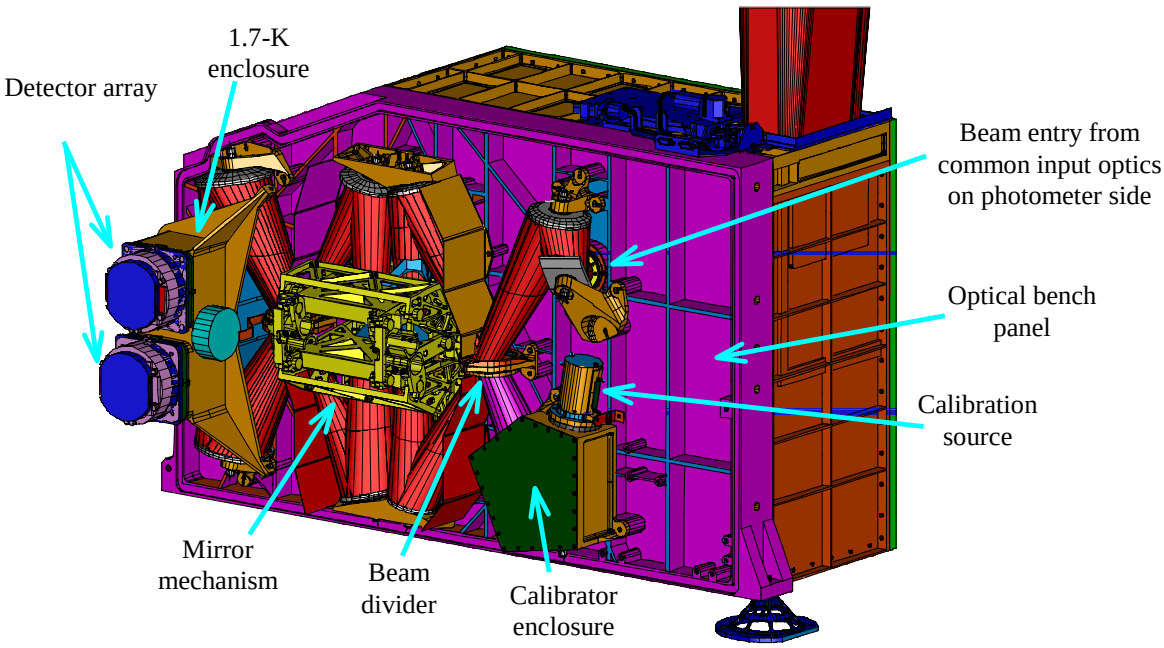

Figure 6: Computer-generated image of the SPIRE FTS layout. The FTS mechanism and the majority of its optics are mounted on the 4.5-K optical bench panel.

The pick-off mirror (located at the intermediate field image on the photometer side of the optical bench panel) sends the spectrometer field of view through a hole in the panel into the FTS side of the instrument. A pupil stop is located between the pick-off mirror and the input fold mirror. The input relay mirror focuses the beam to an intermediate image plane located just after the first beam divider, after which the beam is collimated sent to the moving roof-top assembly. The roof-top mirror shifts the beam and sends it towards the camera mirror, which produces an image plane just before the output beam divider. A pupil image is located near the final fold mirror, making this a convenient location for the entrance aperture to the 1.7-K enclosure. This pupil moves when the optical path difference changes,

so it is not a good place for a limiting cold stop. Instead, the limiting aperture is located at the 4.5-K pupil between the pick-off mirror and the input fold mirror. The output relay mirror focuses the beam onto the detector arrays. Each array has a correcting lens incorporated into its 300-mK filter stack to correct for the non-telecentric FTS optics and provide more uniform fringe contrast and efficiency across the field.

Filters: A filtering scheme similar to the one employed for the photometer channel is used to restrict the passband of the instrument. Filters on the bolometer arrays themselves define the passband for each array. The passbands of the arrays are defined by a combination of edge filters and the cut-off wavelengths of the feedhorn output waveguides. The bands are designed to cover 200 - 325 μm (SSW) and 315 - 670 μm (SLW) at the 90% level. The nominal overlap between the bands is 10 μm at the 90% level, and the actual overlap will be at least 3 μm even in the worst case if the filter edge wavelengths and waveguide diameters are at the extreme ends of their tolerances.

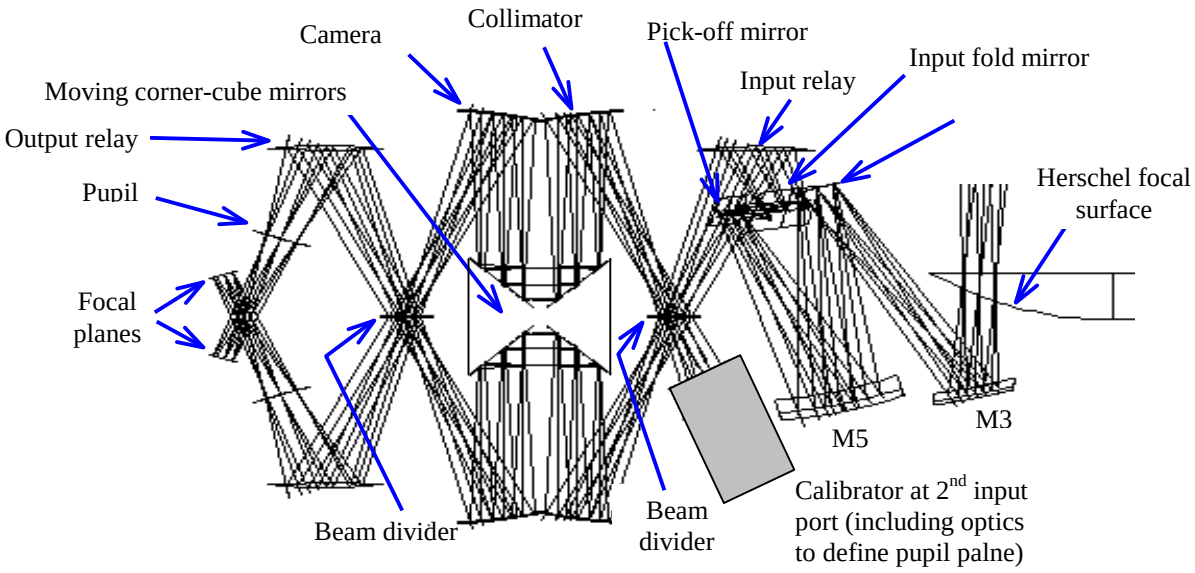

Figure 7: Optical design of the FTS.

FTS detector arrays: The two FTS arrays contain 37 hexagonally close-packed detectors in the short-wavelength array (SSW) and 19 in the long-wavelength (SLW) array. The detector modules will be similar to those used for the photometer, with a mechanical interface to the wall of the 1.7-K enclosure. The layout of the FTS arrays is shown in Fig. 8. The detectors on the periphery of the arrays are partly vignetted by the 2.6-arcminute field of view admitted by the instrument optics (indicated by the large circles in Fig. 8). The short-wavelength array feedhorns are sized to give $2F\lambda$ pixels at 225 μm and the long-wavelength horns to give $2F\lambda$ pixels at 389 μm. This arrangement, although slightly non-optimal from the point of view of point source sensitivity at the central wavelengths of the two arrays, has the advantage that there are numerous co-aligned pixels in the combined field of view. This maximises the observing efficiency for measuring a point source spectrum together with its surrounding sky background and also provides redundancy to the spectrometer in the case of failure of a single pixel within one array. The feedhorn and detector cavity geometry designs have been carefully optimised to provide good sensitivity across the whole wavelength range of the FTS - further details may be found in Rownd et al.[11]

4.3 SPECTROMETER OPERATING MODES

The spectral resolution can be adjusted between 0.04 and 2 cm^{-1} ($\lambda/\Delta\lambda$ = 1000 - 20 at 250 μm), by varying the length of the scan. For spectral mapping of extended sources, the beam steering mirror will be used to provide the necessary pointing changes between scans. The FTS can be operated in two modes: continuous scan or step-and-integrate.

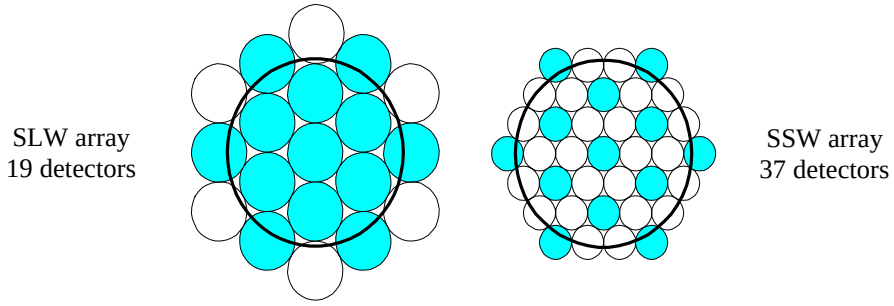

Figure 8: Spectrometer detector arrays. The shaded detectors are co-aligned on the sky in the two bands.

Continuous scan: In this mode the beam steering mechanism is not operating and the scan mirror is moved at constant speed (nominally 0.5 mm s^{-1}) to modulate the signal. The scan mirror control system uses a digital feedback loop to provide a constant speed over the scan length, with an accuracy requirement of 1% (goal 0.5%). The radiation frequencies to be detected are encoded as audio frequencies in the range 3-10 Hz at the detector output. The detectors are read out asynchronously with the samples time-stamped to match them to the corresponding mirror locations. The maximum scan length is 3.5 cm, giving an optical path difference of 14 cm taking into account the factor of four folding in the FTS optics). To ensure that mechanism jitter noise is well below the photon noise level, a relative accuracy of 0.1 μm is required for the mirror position. In order to null the strong telescope background, the FTS calibration source will be on continuously.The mechanism is scanned over the required range with the velocity controlled by the drive electronics and the scan is repeated until the desired total integration time has been reached.

Step-and-integrate: In this mode, the scan mirror is placed sequentially at a range of positions to compete a scan. A step size of 20 μm or less is needed to ensure good over-sampling of the interferogram (corresponding to < 5 μm physical travel). The scan is repeated until the desired total integration time has been reached. The reference source does not need to operate because the telescope background is chopped out by the beam steering mechanism.

In principle, Step-and-Integrate provides higher S/N as the calibrator does not need to be operating, reducing photon noise by a factor of √2. However, Continuous Scan is usually the chosen mode for an FTS as it minimises the effects of 1/f noise and reduces the time overhead associated with moving the mirror between positions. It also has the advantage that the source measurement is referenced against the known internal calibrator rather than an adjacent region of the sky. Step-and-Integrate may be more suited for low resolution observations if the mechanism velocity control does not meet its stringent stability requirement (dictated by the spectrophotometry mode, in which the spectral information is encoded in the sharp central maximum of the interferogram). Which mode is better in practice will depend on the overall performance and noise characteristics of the system and the type of observation. Step-and-Integrate may be the optimum mode for low resolution spectrophotometry and Continuous Scan for higher resolution line spectroscopy.

No on-board processing needs to be done on the FTS data in either mode - all raw interferograms can be telemetered to the ground within the available 130 kbs data rate.

5 ^{3}He COOLER AND 0.3-K THERMAL STRAPS

The same ^{3}He cooler design[12] will be used for both the SPIRE and PACS instruments. It uses porous material to adsorb or release a gas when cooled or heated. This type of refrigerator is well-suited to space operation. Gas gap heat switches are used the control the cooler and there are no moving parts. It can be recycled indefinitely with over 95% duty cycle efficiency and the lifetime is only limited by that of the cold stage from which it is run (in this case, the Herschel cryostat). The evaporation of ^{3}He naturally provides a very stable operating temperature under constant heat load over the entire cycle. The cooler needs no mechanical or vacuum connections and only low-current electrical leads for its operation, making the mechanical and electrical interfaces very simple. For zero-g operation two aspects

of the design have been addressed: liquid confinement and the structural strength required for the launch. The confinement within the evaporator is provided by a porous material which holds the liquid by capillary attraction. For the thermal isolation and structural support of the refrigerator elements, a suspension system using Kevlar wires has been designed to support the cooler firmly during launch whilst minimising the parasitic heat load. The base-line SPIRE cooler contains 4 STP litres of ^{3}He, fits in a 200 x 100 x100 mm envelope and weighs about 0.5 kg. Its performance has been analysed using the same methods that successfully predicted the performance of the IRTS cooler on orbit. When operated from a 1.8-K heat sink it achieves a temperature of 274 mK at the evaporator with a 10-μW load on the evaporator, a hold time of 46 hours and a duty cycle efficiency of 96%. The total time-averaged power load on the 1.7 K heat sink is approximately 3 mW. Copper thermal straps are used to connect the cooler 0.3-K stage to the five detector arrays, and are held rigidly at various positions by Kevlar support modules. The supports units at the entry points to the spectrometer and photometer 1.7-K boxes are also designed to be light-tight. The cooler and thermal strap system constitute a single point failure for the instrument, and great care has been taken in thermal/mechanical design to ensure a robust and reliable system.

6 INSTRUMENT PERFORMANCE ESTIMATION

The sensitivity of SPIRE has been estimated under the assumptions listed below in Table 1. Pessimistic overall optical efficiencies of 30% for the photometer and 15% for the FTS are assumed, taking into account all losses including filter transmission, mirror reflectivity, diffraction within the instrument and pupil alignment errors.

Telescope	Temperature (K)	80		
	Emissivity	0.04		
	Used diameter (m)	3.29		
	No. of observable hours per 24-hr period	21		
Photometer	Bands (μm)	250	363	517
	Numbers of detectors	139	88	43
	Beam FWHM (arcsec.)	17	24	35
	Bolometer Detective Quantum Efficiency	0.73	0.68	0.61
	Feed-horn + cavity + bolometer overall efficiency	0.60	0.65	0.70
	Filter widths ($\lambda/\Delta\lambda$)	3.0	3.2	3.0
	Throughput	λ^2		
	Bolometer yield	0.8		
	Field of view (arcmin.)	4 x 8 (scan map); 4 x 4 (field map)		
	Overall instrument transmission	0.3		
	Reduction in telescope background by cold stop (4)	0.8		
FTS	Bands (μm)	200-325	315-670	
	Numbers of detectors	37	19	
	Bolometer Detective Quantum Efficiency	0.70	0.65	
	Feed-horn + cavity + bolometer overall efficiency	0.70	0.65	
	Maximum spectral resolution (cm^{-1})	0.04		
	Overall instrument transmission	0.15		
	Signal modulation efficiency	0.5		
	Observing efficiency	0.8		
	Electrical filter efficiency	0.8		

Table 1: Assumptions for sensitivity estimation.

The nominal background power levels on the detectors (which are dominated by the telescope emission), and the corresponding photon noise limited NEP values are given in Table 2 and the instrument sensitivity is summarised in Table 3.

		Photometer band (μm)			**FTS band (μm)**	
		250	360 μm	520 μm	200-325	315-670
Background power/detector	pW	3.8	3.0	2.6	11	11
Background-limited NEP	W $Hz^{-1/2}$ x 10^{-17}	7.9	5.9	4.6	11	14

Table 2: Background power and photon noise-limited NEPs for SPIRE.

Photometry				
λ μm		250	360	520
ΔS(5-σ; 1-hr) mJy	Point source (7-point mode)	2.4	2.8	3.1
	4' x 4' jiggle map	8.5	9.3	9.7
	4' x 8' scan map	6.8	7.4	7.7
Time (days) to map 1 $deg.^2$ to 3 mJy 1-σ	1^o x 1^o scan map	1.7	2.0	2.1

Line spectroscopy $\Delta\sigma$ = 0.04 cm^{-1}				
λ μm		200 - 315	315 - 500	500-670
ΔF (5-σ; 1-hr) W m^{-2} x 10^{-17}	Point source	4.7	4.0	4.0 - 5.6
	2.6' map	13	11	11 - 15

Low-resolution spectrophotometry $\Delta\sigma$ = 1 cm^{-1}				
λ μm		200 - 315	315 - 500	500-670
ΔS (5-σ; 1-hr) mJy	Point source	160	140	140 - 190
	2.6' map	430	360	360-500

Table 3: Estimated sensitivity of SPIRE for photometry, line spectroscopy, and low-resolution spectrophotometry.

The extragalactic confusion limit for SPIRE is in the region of 10-20 mJy (depending on the band, the adopted source count models, and how one chooses to define the confusion limit). The photometer is thus capable of integrating down to the Herschel confusion limit with a sensitivity of 5 σ in a matter of ~ 15 minutes, allowing large area confusion-limited surveys to be carried out at a rate on the order of 0.5 square degrees per day. The FTS will be used to follow up brighter sources from this survey (and other existing catalogues) to determine the SEDs and carry out spectral line surveys with simultaneous coverage of the 200 - 670 μm band.

7 THE SPIRE CONSORTIUM

SPIRE is being built by a consortium of European, American and Canadian scientists from the following groups: Caltech/Jet Propulsion Laboratory, Pasadena; CEA Service d'Astrophysique, Saclay, France; Cardiff University, UK; Institut d'Astrophysique Spatiale, Orsay, France; Imperial College, London, UK; Instituto de Astrofisica de Canarias, Tenerife, Spain; Istituto di Fisica dello Spazio Interplanetario, Rome, Italy; Laboratoire d'Astronomie Spatiale, Marseille; Mullard Space Science Laboratory, Surrey, UK; NASA Goddard Space Flight Center, Maryland, USA; Observatoire de Paris, Meudon, Paris; UK Astronomy Technology Centre, Edinburgh, UK; Rutherford Appleton Laboratory, Oxfordshire, UK; Stockholm Observatory, Sweden; Università di Padova, Italy; University of Lethbridge, Canada.

8 ACKNOWLEDGEMENTS

Many people have contributed to the technical definition of SPIRE addressed in this paper, including: Peter Ade, Philippe André, Jean-Louis Augueres, Jean-Paul Baluteau, Jamie Bock, Chris Brockley-Blatt, Terry Cafferty, Martin Caldwell, Christophe Cara, Riccardo Cerulli, John Coker, Patrick Collins, Dustin Crumb, Colin Cunningham, Pascal Dargent, Gary Davis, John Delderfield, Iris Didschuns, Kjetil Dohlen, Lionel Duband, Roger Emery, Didier Ferrand, Alberto Franceschini, Walter Gear, Jason Glenn, Doug Griffin, Peter Hargrave, Peter Hamilton, Martin Harwit, Vic Haynes, Raul Hermoso, Len Husted, David Henry, Viktor Hristov, Don Jennings, Ken King, Brian Kiernan, Andrew Lange, Jerry Lilienthal, Francoise Loubere, Bruno Maffei, Jerome Martignac, Guy Michel, Harry Morgan, Harvey Moseley, Anthony Murphy, David Naylor, Hien Nguyen, Göran Olofsson, Seb Oliver, Renato Orfei, Ian Pain, Ismael Perez-Fournon, Frederic Pinsard, Giampaolo Pisano, Dominique Pouliquen, Faiz Rahman, Tony Richards, Louis Rodriguez, Michael Rowan-Robinson, Brooks Rownd, Paolo Saraceno, Srinivasan Sethuraman, Dave Smith, Brian Stobie, Rashmi Sudiwala, Kalyani Sukhatme, Joe Taylor, Carole Tucker, Anthony Turner, Berend Winter, Adam Woodcraft, Gillian Wright.

9 REFERENCES

1. G. Pilbratt, “Introduction to the Herschel Space Observatory”, Proc. SPIE 4850 (this volume), Kona, 24-28 August 2002.
2. I. Smail, R. Ivison, A. Blain, and J.-P. Kneib, "Deep sub-mm surveys with SCUBA. In *After the Dark Ages: When Galaxies were Young (the Universe at 2 < z < 5)*, American Institute of Physics Press, p. 312, 1999.
3. M. Griffin, B. Swinyard, and L. Vigroux, " The SPIRE instrument for FIRST", Proc. SPIE 4013, 184, 2000.
4. K. Dohlen, A. Orignéa, D. Pouliquen, and B. Swinyard, "Optical design of the SPIRE instrument for FIRST", Proc. SPIE 4013, 119, 2000.
5. P. Hargrave, J.W. Beeman, P.A. Collins, I. Didschuns, M.J. Griffin, B. Kiernan, G. Pisano, and R. Hermoso, "In-flight calibration sources for Herschel-SPIRE", Proc. SPIE 4850 (this volume), Kona, 24-28 August 2002.
6. I. Pain, G.S. Wright, and B. Stobie, "SPIRE beam steering mirror: a cryogenic two-axis mechanism for the Herschel Space Observatory", Proc. SPIE 4850 (this volume), Kona, 24-28 August 2002.
7. A.D. Turner, J.J. Bock, H.T. Nguyen, S. Sethuramam, J.W. Beeman, J. Glenn, P.C. Hargrave, A.L. Woodcraft, V.V. Hristov, and F. Rahman, "Si_3N_4 micromesh bolometer array for sub-millimeter astrophysics", Applied Optics 40, 4921, 2001.
8. W.S. Holland, E.I. Robson, W. K. Gear, C.R. Cunningham, J.F. Lightfoot, T. Jenness, R.J. Ivison, J.A. Stevens, P.A.R. Ade, M.J. Griffin, W.D. Duncan, J.A. Murphy, and D.A. Naylor 1999, "SCUBA: a common-user submillimetre camera operating on the James Clerk Maxwell Telescope", Mon. Not. R. Astron. Soc. 303, 659-672, 1999.
9. B.M. Swinyard, D. Ferrand, D. Pouliquen, J.-P. Baluteau, P. Dargent, K. Dohlen, P.A.R. Ade, M.E. Caldwell, and M.J. Griffin, “Imaging FTS for Herschel-SPIRE”, Proc. SPIE 4850 (this volume), Kona, 24-28 August 2002.
10. P.A.R Ade, P.A. Hamilton, and D.A. Naylor. "An absolute dual beam emission spectrometer", Fourier transform spectroscopy: new methods and applications, OSA, 90, 1999.
11. B. Rownd, J. Glenn, J.J. Bock, G. Chattopadhyay, and M.J Griffin, "Design and performance of feedhorn-coupled arrays coupled to submillimeter bolometers for the SPIRE instrument aboard the Herschel Space Observatory", Proc. SPIE 4855, Kona, 24-28 August 2002 (in press).
12. L. Duband, “Spaceborne helium adsorption coolers”, *Proceedings of ESA Symposium on The Far Infrared and Submillimetre Universe*, Grenoble, 15-17 April 1977, ESA SP-401, 357, 1997.